Journal of the Association of Arab Universities for Basic and Applied Sciences (2014) **15**, 15–20

University of Bahrain

**Journal of the Association of Arab Universities for Basic and Applied Sciences**

www.elsevier.com/locate/jaaubas
www.sciencedirect.com

# خواص التوصيل الكهربائي والكهروحراري لشرائح أوكسيد القصدير الرقيقة ذات التركيب النانوي

م. أ. بطل، غسان ناشد، فارس حاج جنيد

قسم الفيزياء، كلية العلوم، جامعة حلب، سورية

**الملخص:**

رُسبت شرائح رقيقة من أوكسيد القصدير المطعم بالحديد والنحاس على مساند من الزجاج وأوكسيد الألمنيوم وذلك باستخدام طريق تقنية الطلاء بالتغطيس في المحلول الجيلاتي، مَسند أوكسيد الألمنيوم حُضّر بطريقة الترسيب الكهربائي، والعينات المرسبة عُوملت حرارياً عند درجة حرارة 600°C لمدة ساعتين. بينت قياسات طيف حيود الأشعة السينية بأن العينات المرسبة ذات تركيب متعدد البلورات وبانعكاسات تشير الى تكون اوكسيد $SnO_2$ ذو طور كاسيترايت. وباستخدام قياس خواص التيار والفولتية (I–V) عند درجات الحرارة المختلفة للعينات المحضرة على مسند من الزجاج، فان كثافة الحالات الالكترونية عند سطح فيرمي قد تم حسابها. كما ان الاثر الكهروحراري عند تغير درجة الحرارة للعينات المحضرة تحت ضغط منخفض يقدر بـــ1 ملي بار قد تم قياسه ومن خلال ذلك أمكن تحديد معامل سيبك، تركيز حاملات التيار، وحركيتها وكذلك معامل النوعية. لقد تم معرفة بأن معامل سيبك يتحسن عندما تكون الطبقة الساندة للشرائح هي أوكسيد الألمنيوم.

Journal of the Association of Arab Universities for Basic and Applied Sciences (2014) **15**, 15–20

University of Bahrain

**Journal of the Association of Arab Universities for Basic and Applied Sciences**

www.elsevier.com/locate/jaaubas
www.sciencedirect.com

ORIGINAL ARTICLE

# Conductivity and thermoelectric properties of nanostructure tin oxide thin films

**M.A. Batal, Ghassan Nashed, Fares Haj Jneed** *

*Department of Physics College of Science, University of Aleppo, Syria*

Received 3 May 2012; revised 3 August 2012; accepted 17 September 2012
Available online 6 June 2013

**KEYWORDS**

Thin films;
$SnO_2$;
Seebeck effect;
Thermoelectric

**Abstract** Tin oxide thin films doped with iron or copper were deposited on glass and porous alumina substrates, using the co-deposition dip coating sol–gel technique. Alumina substrate was prepared by the anodizing technique. Samples were sintered for 2 h at temperature 600 °C. The XRD spectrum of deposited samples shows a polycrystalline structure with a clear characteristic peak of $SnO_2$ cassiterite phase. From (I–V) characteristics measured at different temperatures for samples prepared on glass substrates, the density of states at the Fermi level was calculated. Thermoelectric effect was measured with a change of temperature for prepared samples under low pressure 1 mbar. Seebeck coefficient, the carrier concentration, the charge carrier mobility and the figure merit were determined for prepared samples under low pressure 1 mbar. Seebeck coefficient was improved when films were deposited on porous Alumina substrates.



## 1. Introduction

Thermoelectric phenomenon was first discovered by Thomas J. Seebeck in 1822, when he developed a voltage by joining two pieces of different materials together and placing a temperature difference to the couple. He also found that the voltage difference observed was proportional to the temperature gradient ($S = V/\Delta T$). This effect was named after him and the coefficient $S$ (also known as $\alpha$) is known as Seebeck coefficient. This coefficient is very low for metals (only a few mV/$K$) and much larger for semiconductors (typically a few 100 mV/$K$). The aptitude of a material for thermoelectric applications is determined by using a dimensionless figure of merit (Pichanusakorn et al., 2010):

$$ZT = \frac{S^2\sigma}{\kappa}T$$

in which $S$, $\sigma$, $T$ and $\kappa$ are, respectively, Seebeck coefficient, electrical conductivity, operating temperature and total thermal conductivity. Thermoelectric energy conversion, which directly transforms the heat into electricity, has drawn much attention in recent years and found applications in a variety of areas such as renewable and clean energy, thermoelectric power generation, small scale cooling systems for electronic devices, microrefrigerator devices, and micro-thermo-chemistry on a chip for microelectronic components (Fahrettin, 2009).The thermoelectric materials are usually bulk, thin film and low-dimensional structures such as Skutterudite

* Corresponding author. Tel.: +963 955158906.
E-mail address: fareshaj@gmail.com (F.H. Jneed).
Peer review under responsibility of University of Bahrain.

Production and hosting by Elsevier

1815-3852 © 2013 Production and hosting by Elsevier B.V. on behalf of University of Bahrain.
http://dx.doi.org/10.1016/j.jaubas.2012.09.005

type ($CoAs_3$-type) alloys. Since thin films are expected to have lower thermal conductivity than the bulk materials, due to strong phonon scattering at their interfaces, thermoelectric films likely open up the possibility for improvement of thermoelectric efficiency (Frank, 2007). Although some thermoelectric materials, such as $Bi_2S_3$ and $Bi_2Te_3$ films, have found particular applications, their efficiencies at the best ($ZT \sim 1$) are not enough for wider utilization in commercial applications (Banerjee et al., 2004). Thus, development of materials with high thermoelectric efficiencies is one of the main current research interests. Tin oxide ($SnO_2$) thin film is well known as a wide band gap n-type semiconductor ($E_g$ = 3.6–3.8 eV) with high simultaneous electrical conductivity and optical transparency in visible region of the spectrum (Bulusua et al., 2008). So far, there are only a few reports on thermoelectric properties of $SnO_2$ thin films. In this paper, we report the preparation of p-type $SnO_2$ doped with Fe or Cu thin films with a large thermoelectric efficiency to improve the thermoelectric effect of $SnO_2$ doped with Fe or Cu thin films (Bagherim et al., 2009). The thermoelectrical, electrical and structural properties of these films are studied using Seebeck effect measurements.

## 2. Experimental

The $SnO_2$:Fe or $SnO_2$:Cu thin films have been prepared on glass and porous alumina substrates prepared by the anodizing technique, using the co-deposition dip coating sol–gel technique, the films were doped with iron or copper at concentration %5. $SnCl_4.5H_2O$ and $FeCl_3$:$6H_2O$ or $CuCl_2.2H_2O$ were purchased from MERCK company and are used as starting materials. Typically, $SnCl_4.5H_2O$ and $FeCl_3$:$6H_2O$ or $CuCl_2.2H_2O$ are mixed together in Ethanol. The obtained solution is continuously stirred at 80 °C for 4 h and aged 2 days.

Glass and porous alumina substrates were dipped in the sol–gel and then drawn from it at the speed of 7 cm/min. Then dried at 80 °C, and sintered at 600 °C for 2 h.

## 3. Structural characterization of films

XRD patterns of $SnO_2$ doped with Fe or Cu films deposited on glass substrates were recorded by Philips system using Cu Kα ($\lambda$ = 0.154056 nm) radiation with $2\theta$ in the range of 20–70° as shown in Fig. 1.

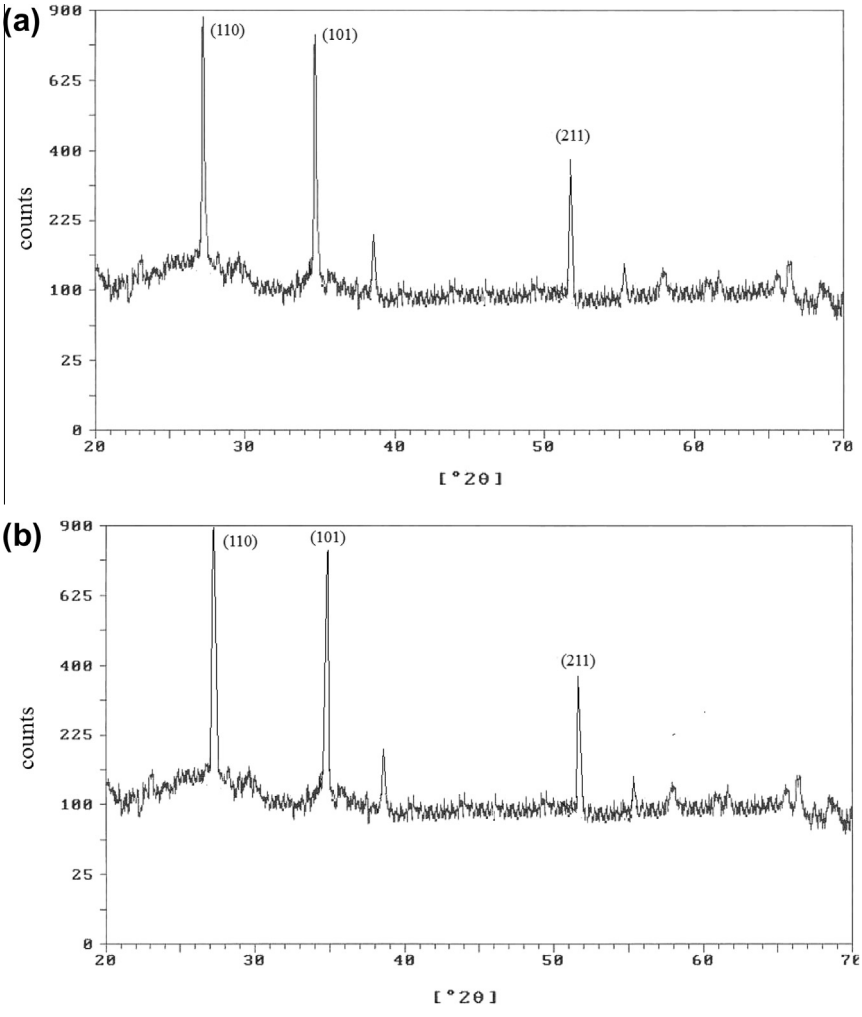


**Figure 1** XRD pattern of prepared films deposited on glass substrates (a) $SnO_2$ doped with Fe (b) $SnO_2$ doped with Cu.

**Table 1** Summary of the XRD parameters and crystallite size mean grain size of samples for peak (110).

| Peak | Crystallite size (nm) |
|---|---|
| $SnO_2$ (Timonah and Chunhui, 2010) | 30 |
| $SnO_2$:Fe | 19.75 |
| $SnO_2$:Cu | 26.57 |

From the XRD spectrum, the films polycrystalline in nature have all peaks corresponding to the specific planes with a maximum intensity peak from (110) planes. The relative intensity of all XRD peaks decreases in $Fe^{3+}$ or $Cu^{+2}$ doped films which can be attributed to incorporation of $Fe^{3+}$ or $Cu^{+2}$ ions into the $SnO_2$ lattice, if it is compared with pure $SnO_2$ XRD spectrum, and the resultant decrease of crystallite size. This is also evidenced by the increase in the full width at half maxima (FWHM) of the XRD peaks with an increase in $Fe^{3+}$ or $Cu^{+2}$ doping in the $SnO_2$ films. This reduction of crystallite size with an increase in $Fe^{3+}$ or $Cu^{+2}$-doping in the films has been discussed in the past by some researchers, for example, Fang et al. explained that the $Fe^{3+}$ or $Cu^{+2}$ portion formed stable solid solutions with $SnO_2$, occupying regular lattice site in $SnO_2$ and introducing point defects which caused changes in stoichiometry due to charge imbalance. Furthermore, the fact that $Fe^{3+}$ or $Cu^{+2}$ ion has smaller radius than $Sn^{+4}$ ion, $SnO_2$ doping with $Fe^{3+}$ or $Cu^{+2}$ should result in a contraction of the lattice parameters (Timonah et al., 2010). The average crystalline size was calculated using Scherrer's formula based on the XRD patterns (Timonah et al., 2010):

$$D = k\lambda/(\delta w \cos\theta) \quad (1)$$

where $D$ is the average crystalline (grain) size, $k$ is a constant ($\sim$1), $\lambda$ is the X-ray wavelength and its value is 0.154 nm, $\delta w$ is the full width at half maximum of XRD peaks and $\theta$ is the Bragg angle. Table 1 shows average crystalline (grain) size of the prepared films.

## 4. Atomic force microscopy

Fig. 2 shows AFM images for $SnO_2$ doped with Fe and Cu deposited on glass substrates respectively we note that the grain size is nano order and it fits well with crystalline size measured by XRD.

## 5. (I–V) Characteristic

DC measurements were carried out using a high resistance meter (hp 4339A). I–V characteristics were taken at constant temperature (150, 200, 250 °C) for samples deposited on glass substrate. The (I–V) characteristics of the $SnO_2$:Fe or $SnO_2$:Cu at different temperatures are shown in Fig. 3. The I–V curves indicate two regions (I and II). At lower voltages (region I), the

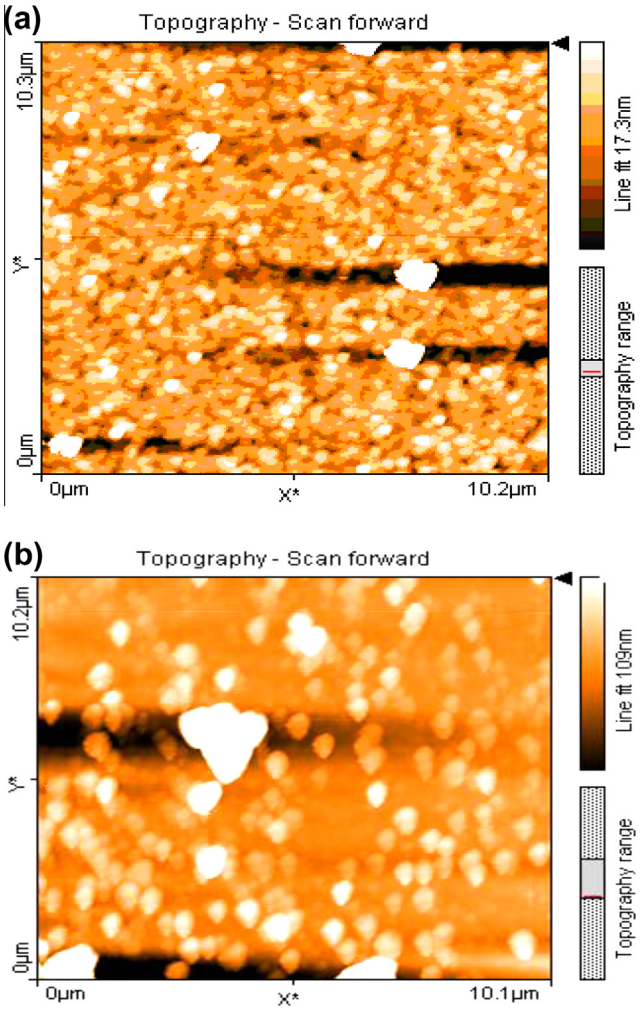


**Figure 2** AFM images of prepared films deposited on glass substrates (a) $SnO_2$ doped with Fe (b) $SnO_2$ doped with Cu.

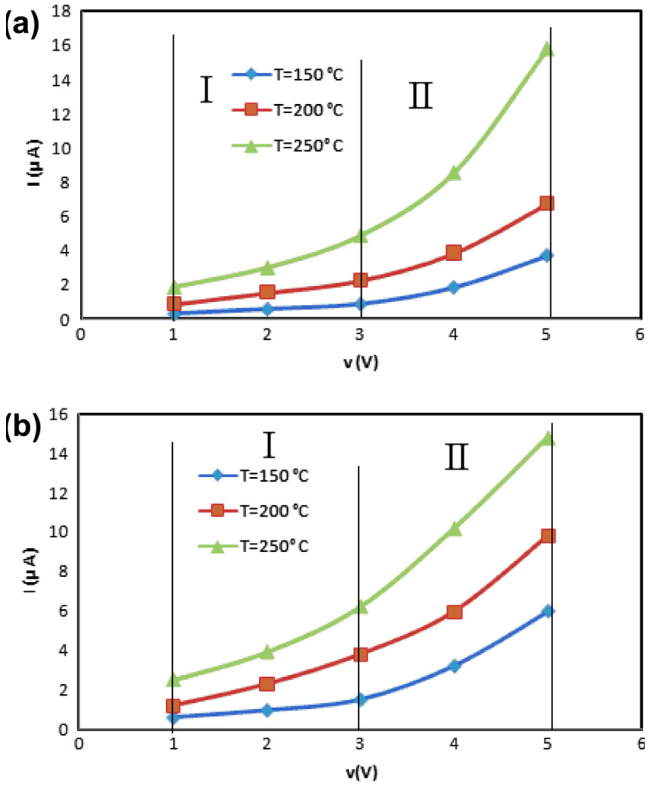


**Figure 3** The variation of the carrier concentration with temperature (a) $SnO_2$ doped with Fe (b) $SnO_2$ doped with Cu.

**Table 2** Density of states at the Fermi level of samples.

| N(EF) ($eV^{-1}m^{-3}$) | $T$ = 150 °C | $T$ = 200 °C | $T$ = 250 °C |
|---|---|---|---|
| $SnO_2$:Fe | 1.77944E + 19 | 1.33571E + 20 | 1.25162E + 21 |
| $SnO_2$:Cu | 2.65025E + 19 | 3.47235E + 19 | 8.73979E + 19 |

**Table 3** Activation energy for all samples at region I and II.

| $E_a$ (eV) | Region (1) | Region (2) |
|---|---|---|
| $SnO_2$:Fe | 0.2827 | 0.1727 |
| $SnO_2$:Cu | 0.3286 | 0.1795 |

conduction is ohmic, i.e., the current changes linearly with voltage, but, at higher voltages (region II), the conduction is nonohmic.

The slope of the second region II increases with increasing temperature. This confirms the presence of space charge limited conductivity, i.e., high-electric conductivity region is governed by the injected space charge. The density of states at the Fermi level can be determined using the following relation (Fahrettin, 2009):

$$N(E_F) = \frac{2\varepsilon_r \varepsilon_0 \Delta V}{ed^2 \Delta E_F} \quad (2)$$

Since:

$$\Delta E_F = kTLn\frac{I_2 V_1}{I_1 V_2} \quad (3)$$

where $\Delta E_F$ is the shift of the quasi-Fermi level, $\Delta V$ is the change of applied voltage, $e$ is the electronic charge, $\varepsilon_r$ is the dielectric constant of the material (9.65 of $SnO_2$), $d$ is the film thickness and $k$ is the Boltzmann constant. Table 2 shows the density of states at the Fermi level of samples.

The electrical conductivity is dependent on temperature of the $SnO_2$ doped with Fe or Cu films. It can be analyzed by the following relation (Fahrettin, 2009):

$$\sigma = \sigma_0 \exp\left(-\frac{E_a}{kT}\right) \quad (4)$$

where $E_a$ is the activation energy, $T$ is the temperature, $k$ is the Boltzmann constant and $\sigma_0$ is the pre-exponential factor. The electrical conductivity of the film increases with the increase of temperature.

Activation energy values for regions (I) and (II) were determined from the slope $Ln\sigma = f\left(\frac{1}{T}\right)$ as shown in Table 3.

Table 3 shows activation energy at lower voltages (region I) is larger than at higher voltages (region II).

## 6. Thermoelectric properties

The chamber in which the sample was tested was initially pumped using a rotary pump to a rough vacuum of 1 mbar.

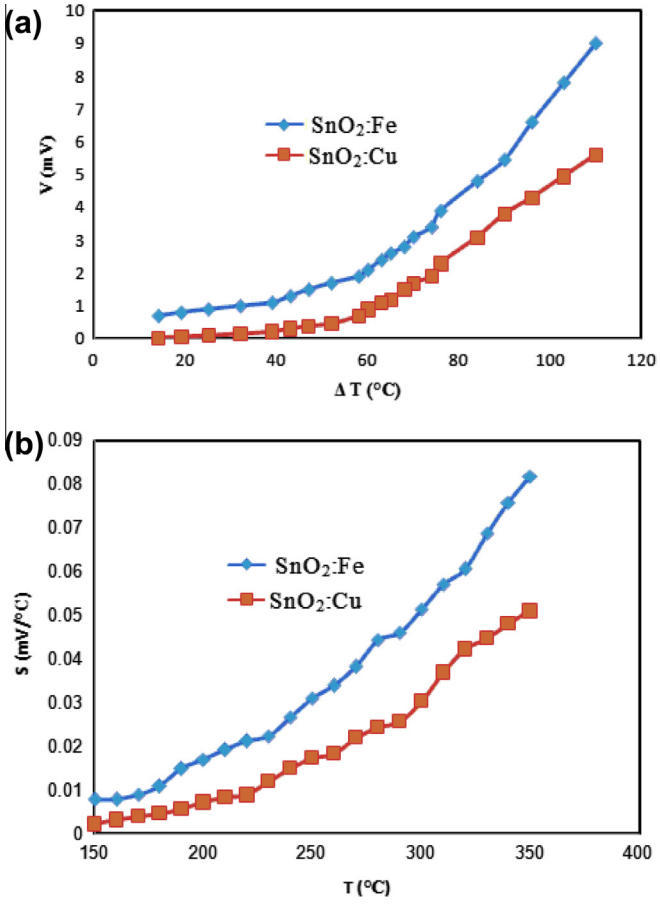


**Figure 4** (a) The variation of the potential with Temperature difference, (b) the variation of the Seebeck coefficient with temperature.

The difference in temperature at the two ends of the sample was measured by placing two thermocouples at the ends of the sample. In order to create a temperature gradient along with the sample, only one end of the sample was heated leading to the creation of a hot junction and a cold junction. One of the thermocouples measures the temperature at the hot junction of the sample, whereas the other thermocouple measures the temperature at the cold junction.

A graph of the measured thermoelectric against temperature difference was plotted, Fig. 4a, and the slope of the curve thus obtained gives the Seebeck coefficient of the film Fig. 4b. The Seebeck coefficient of the deposited films was found to be positive confirming to the p-type behavior of tin oxide doped with iron or copper.

The Seebeck coefficient, $S$ dependence on the temperature are shown in Fig. 4. In the extrinsic conductivity region, the increase in thermoelectric power with temperature is due to the increasing number of thermally excited carriers. The Seebeck coefficient of the film increases with increasing temperature and indicates two linear regions. The p-type electrical conductivity of the $SnO_2$ doped with iron or copper film originates from ionized defects (Batzill et al., 2005). The sign positive of Seebeck coefficient increases with increasing temperature due to the high mobility of minority carriers. In the oxide semiconductors with low mobility, the charge carriers are localized at vacant sites and the conductivity takes place via a hopping process. Therefore, the carrier concentration for the $SnO_2$ doped Fe or Cu films is described as follows:

$$n = N\exp\left(-\frac{Se}{k}\right) \tag{5}$$

where $e$ is the electron charge, $k$ is the Boltzmann constant, $S$ is the Seebeck coefficient and $N$ is the density of states.

The carrier concentration for the $SnO_2$ film was determined as a function of temperature using Eq. (5) and is shown in Fig. 5a. The n values of the film increase with increasing temperature. The charge carrier mobility is described as follows (Hammad et al., 2011):

$$\mu = \frac{1}{en\rho} \tag{6}$$

Fig. 5b shows the charge carrier mobility dependence on temperature for the $SnO_2$ doped with Fe or Cu film, the mobility increases with an increase of temperature. The increase in mobility with temperature suggests that the hopping conductivity is dominant in the $SnO_2$ doped with Fe or Cu film.

## 7. Seebeck effect improvement of tin oxide films

An ideal thermoelectric material should possess large Seebeck coefficients, high electrical conductivity and low thermal conductivity. High electrical conductivity is necessary in order to minimize Joule heating, while a low thermal conductivity helps to retain heat at the junctions and maintain a large temperature gradient. In metals, the ratio of the thermal conductivity to electrical conductivity is a constant (Wiedemann–Franz-Lorenz law) and it is not possible to reduce one while increasing the other. In semiconductors the ratio of the thermal conductivity to electrical conductivity is greater than in metals owing to their poorer electrical conductivity. This ratio can be decreased (i.e., the electrical conductivity can be

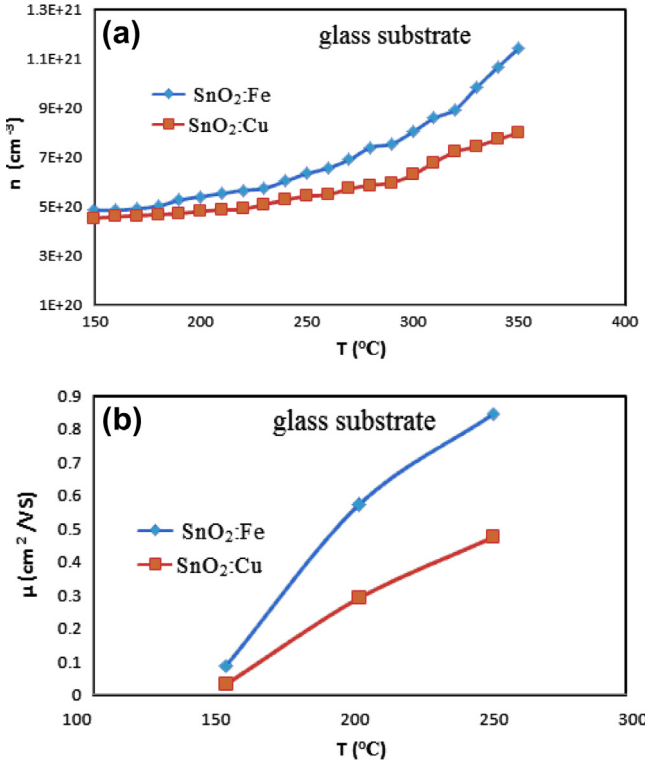


**Figure 5** (a) The variation of the carrier concentration with temperature, (b) variation of charge carrier mobility with temperature.

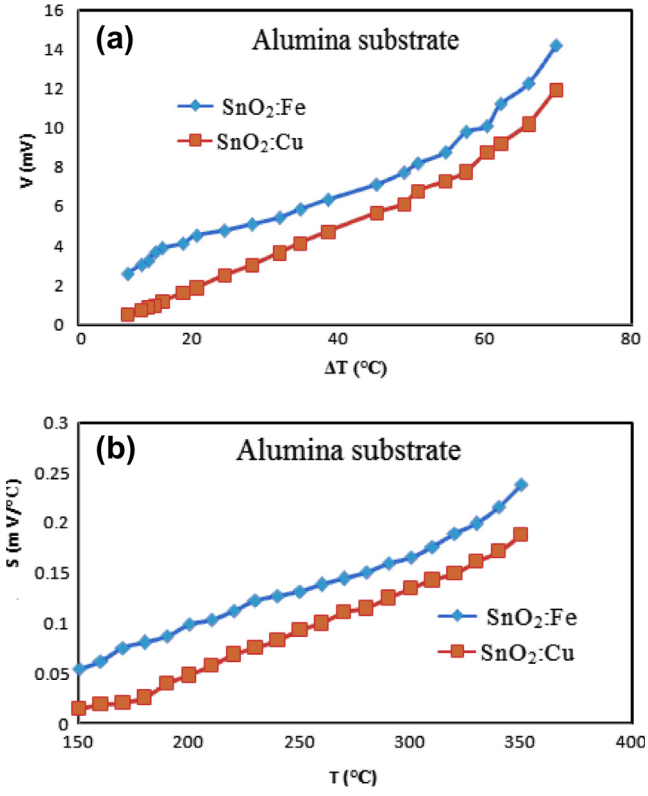


**Figure 6** (a) The variation of the potential with temperature difference, (b) the variation of the Seebeck coefficient with temperature.

increased) if the thermoelectric material is alloyed with an isomorphous element or compound (Shi et al., 2004).

Fig. 6a,b shows the measured thermoelectric potential as a function of temperature difference was plotted and the Seebeck coefficient as a function of temperature for the $SnO_2$:Fe or $SnO_2$:Cu films deposited on porous alumina substrate. The Seebeck coefficient of the deposited films was found to be positive confirming to the p-type behavior of tin oxide doped with iron or copper. Seebeck coefficient for $SnO_2$:Fe is larger than Seebeck coefficient for $SnO_2$:Cu films deposited on glass and alumina substrates. Seebeck coefficient for films deposited on glass substrate is smaller than Seebeck coefficient for films deposited on alumina substrate and this can be understood due to deference thermal and electrical conductivity of substrates.

## 8. Conclusions

In this paper, we have studied the preparation and characterization of the $SnO_2$:Fe or $SnO_2$:Cu thin films with high thermoelectric efficiency. These films have been deposited by using the co-deposition dip coating sol–gel technique. The XRD spectrum of deposited samples shows a polycrystalline structure with a clear characteristic peak of $SnO_2$ cassiterite phase.

The thermoelectrical measurements have shown p-type conductivity in thin films with Fe or Cu. Also, the Seebeck coefficient for $SnO_2$:Fe or $SnO_2$:Cu films deposited on porous alumina substrates prepared by the anodizing technique is larger than Seebeck coefficient for $SnO_2$:Fe or $SnO_2$:Cu films deposited on glass substrates.

## References

Bagherim, M., Shahtahmasebi, N., Alinejad, A., Youssefi, M., Shokooh-Saremi, M., 2009. Fe-doped $SnO_2$ transparent semiconducting thin films deposited by spray pyrolysis technique: thermoelectric and p-type conductivity properties. Solid State Sciences 11, 233–239, Tehran.

Banerjee, N., Maity, R., Kundoo, S., Chattopadhyay, K.K., 2004. Poole–Frenkel effect in nan crystalline $SnO_2$: F thin films prepared by a sol–gel dip-coating technique. Indian Physics 201, 983–989, New Delhi.

Batzill, M., Diebold, U., 2005. The surface and materials science of tin oxide. Progress in Surface Science 79, 47–154, New York.

Bulusua, A., Walkerb, D.G., 2008. Review of electronic transport models for thermoelectric materials. Superlattices and Microstructures 44, 1–36, New York.

Fahrettin, Y., 2009. Electrical conductivity, Seebeck coefficient and optical properties of $SnO_2$ film deposited on ITO by dip coating. Journal of Alloys and Compounds 74, 55–59. Ankara.

Frank, R., MOOS, R., 2007. Direct thermoelectric gas sensors: design aspects and first gas sensors. Sensors and Actuators 123, 413–419, Berlin.

Hammad, T.M., Hejazy, N.K., 2011. Structural, electrical and optical properties of ATO thin films fabricated by dip coating method. International Nano Letters 1, 123–128, Jerusalem.

Pichanusakorn, P., Bandaru, P., 2010. Nanostructured thermoelectrics. Materials Science and Engineering 67, 19–63, New York.

Shi, L., Hao, Q., Yu, C., 2004. Thermal conductivities of individual tin dioxide nanobelts. Applied Physics Letters 84, 2638–2641, Tokyo.

Timonah, N.S., Chunhui, Y.L.S., 2010. Structural, optical and electrical properties of Fe-doped $SnO_2$ fabricated by sol–gel dip coating technique. Materials Science in Semiconductor Processing 13, 113–125, Pekin.